Nonlocal effects on second harmonic generation in low-damping epsilon-near-zero slabs

D. de Ceglia[1], M. A. Vincenti[1], S. Campione[2], F. Capolino[2], M. Scalora[3]
[1]*National Research Council - AMRDEC, Charles M. Bowden Research Laboratory, Redstone Arsenal - AL, 35898 – USA*
[2]*Department of Electrical Engineering and Computer Science, University of California, Irvine – CA, 92697 - USA*
[3]*Charles M. Bowden Research Laboratory, AMRDEC, US Army RDECOM, Redstone Arsenal - AL, 35898, USA*
E-mail:domenico.deceglia@us.army.mil

Abstract: We predict enhanced second-harmonic generation in low-damping epsilon-near-zero slabs made of plasmonic nanoshells. We further discuss the contribution of nonlocal effects induced by free-electron gas pressure in metals to the nonlinear response of the slab.
OCIS codes: (190.0190) Nonlinear optics; (160.3918) Metamaterials; (190.2620) Harmonic generation and mixing.

1. Introduction

Sub-wavelength epsilon-near-zero (ENZ) slabs have been shown to increase the efficiency of harmonic generation processes thanks to the magnification of the electric field within the slab due to satisfaction of boundary conditions at the interfaces with a higher-index substrate [1-3]. This effect occurs when the slab is illuminated through an obliquely-incident plane wave for transverse magnetic (TM) polarization and is due to the continuity of displacement field component perpendicular to the interfaces. Metamaterials offer several solutions to engineer the ENZ condition, for example by exploiting the electric dipole resonance of composite materials made of arrangements of metallic nanoparticles [4]. While it is straightforward to make the real part of the effective permittivity cross zero at least at one frequency, this is not the case for the imaginary part, whose value limits field enhancement and penalizes both linear and nonlinear optical applications [1, 3, 5]. The inclusion of active, gain materials in the metamaterial [6, 7] or the use of low-loss plasmonic materials [8] are promising approaches to mitigate losses. In a low-damping ENZ slab two different channels for the enhancement of nonlinear processes are available: (i) a pseudo-Brewster effect; (ii) the presence of narrow-band resonances associated with leaky modes. We show that, when physical parameters meet one of these conditions, conversion efficiency of second harmonic (SH) generation originated from Lorentz, Coulomb and convective forces acting on free electrons is strongly enhanced. At the same time, we show how inherent nonlocalities due to the free-electron hydrodynamic pressure impact the nonlinear response of the structure.

2. Field Enhancement in low-damping ENZ slabs

The proposed ENZ metamaterial slab comprises a square lattice of nanocylinders with silver nanoshells, with periodicity *a*, as shown in Fig. 1(a). The nanoshells' core is a silica-like host matrix containing active, gain molecules (Rhodamine 800) to compensate losses by lowering the imaginary part of the effective permittivity. The incident field is TM-polarized, i.e., the electric field lies in the plane of incidence *x*-*z* [see Fig. 1(a)].

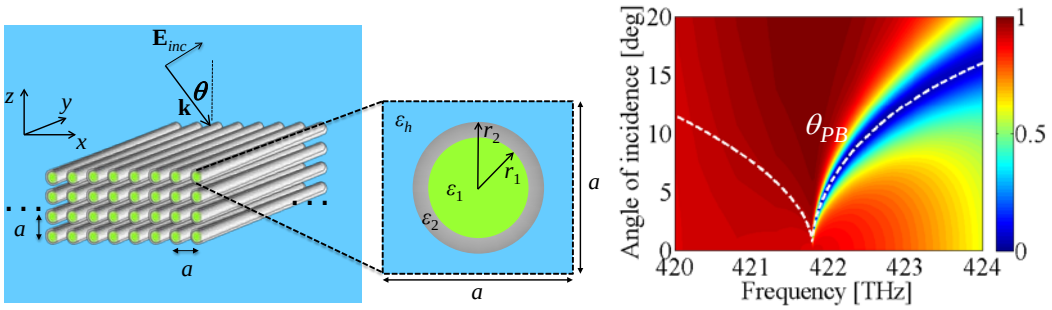

(a) (b)

Fig. 1. (a) Schematic of the ENZ metamaterial slab made of cylindrical nanoshells arranged in a square 2D array (the period is *a*). (b) Reflectance (TM polarization) of a 4-period-thick array of cylindrical nanoshells versus frequency and angle of incidence.

The permittivity of silver ε_2 is taken from [9], while for the permittivity in the core we use the expression $\varepsilon_1 = 2.25 + \varepsilon_c\left(\Gamma_{\text{pump}}, \bar{N}_0\right)$, with $\varepsilon_c\left(\Gamma_{\text{pump}}, \bar{N}_0\right)$ as in [7], assuming dye concentration $\bar{N}_0 = 6.75$ mM and pumping

rate $\Gamma_{pump} = 6.5\times10^{9}$ s^{-1}. The host medium is silica ($\varepsilon_h = 2.25$) and geometrical parameters are $r_1 = 25$ nm, $r_2 = 30$ nm, and $a = 114$ nm. The relative, effective permittivity ε_{eff} of the structure is retrieved via full-wave numerical simulations with the finite element method in COMSOL by using the Nicolson-Ross-Weir (NRW) retrieval method. For this calculation we consider a finite slab of metamaterial with a thickness of 4 periods in the *z*-direction. The structure is designed so as the emission frequency of the dye molecules, i.e., 422 THz, matches the zero-crossing frequency of the real part of the effective permittivity Re[ε_{eff}]. The amount of gain in the nanoshells' core is then chosen in order to lower the imaginary part of the effective permittivity Im[ε_{eff}] at the zero-crossing frequency (~422 THz). As a result, the slab shows an effective permittivity of ~$5\times10^{-4}(1+i)$ at 422 THz. In Fig. 1(b) we show the reflectance from the slab, calculated by homogenizing the structure with the NRW effective permittivity. The ENZ condition causes impedance mismatch at the slab interface so that reflectance at normal incidence is close to 1 around 422 THz. However, a tunneling effect for TM polarized plane waves occurs within a very narrow angular bandwidth centered at the pseudo-Brewster (PB) angle [10], where reflection is drastically inhibited [Fig. 1(b)]. The analytical expression of the PB angle shows good overlap with the minimum reflectance of the slab [dashed line in Fig. 1(b)]. Tunneling at the PB angle is associated with a strong electric field enhancement in the ENZ slab triggered by the continuity of the *z*-component of the displacement field at the interface [1, 3]. We then calculate the average electric field enhancement $\langle|\mathbf{E}|/E_0\rangle$ in the ENZ slab near the PB angle by means of full-wave numerical simulations (COMSOL). Here E_0 is the amplitude of the incident electric field and **E** is the local electric field in the slab. The average field enhancement $\langle|\mathbf{E}|/E_0\rangle$ reaches a peak of 25 near 422 THz for an angle of incidence near 2°, i.e., close to the PB angle. Beside the PB effect, three resonances, associated with leaky modes supported by the ENZ slab, appear in the frequency-angle map for larger angles [see the three bright signatures of these resonances for angles larger than 5° in Fig. 2(a)], where field enhancement reaches values similar to those relative to PB angle.

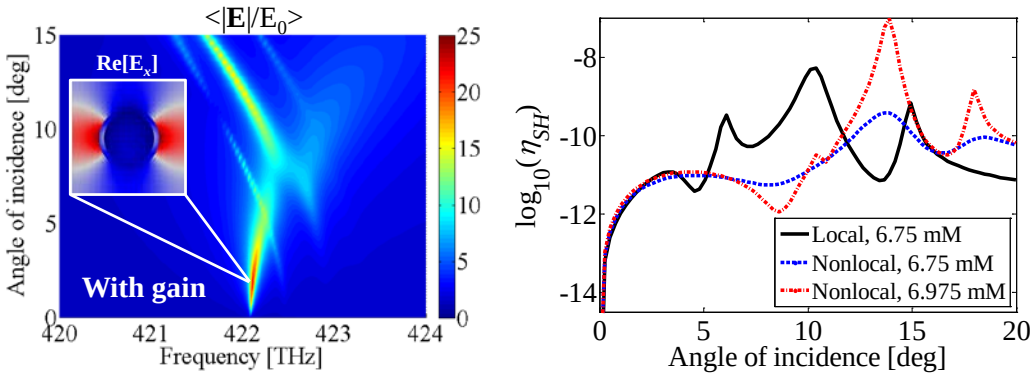

(a) (b)

Figure 2. (a) Electric field enhancement in the ENZ slab averaged over one unit cell of the array. Inset: field localization at the PB angle. (b) SH efficiency from the slab in Fig. 1(a). Black, solid line refers to the local approximation [scenario (i)]; blue, dashed line to the nonlocal scenario (ii) with dye molecules concentration $\bar{N}_0 = 6.75$ mM ; red, dash-dotted line to the nonlocal scenario (iii) with $\bar{N}_0 = 6.975$ mM.

3. Enhancement of second harmonic generation and nonlocal effects

We exploit the strong field enhancement provided by the ENZ slab [Fig. 2(a)] to boost the conversion efficiency of SH generation. We adopt the hydrodynamic model for free electrons to take into account nonlinear and nonlocal effects [11, 12]. Here we assume that a fundamental frequency (FF) signal, tuned at the ENZ frequency (422 THz), impinges on the ENZ slab in Fig. 1 and we calculate the SH signal originating from the metallic nanoshells. The input irradiance at the FF is 100 kW/cm^2. The conversion efficiency of SH generation is evaluated as $\eta_{SH} = P_{SH} / P_{FF}$, where P_{FF} is the input power at the FF and P_{SH} is the total power radiated at the SH frequency (obtained by adding forward and backward radiation). In Fig. 2(b) we plot η_{SH} on a logarithmic scale as a function of the angle of incidence for a pump frequency tuned at 422.2 THz. We consider three different scenarios: (i) local response approximation, in which nonlocal effects are neglected, i.e., Fermi velocity $v_{\text{Fermi}} = 0$ [black line in Fig. 2(b)]; (ii) nonlocal effects are taken into account [blue line in Fig. 2(b)]; (iii) nonlocal effects are taken into account

and the amount of gain in the nanoshells' core is slightly increased from $\bar{N}_0 = 6.75$ mM to $\bar{N}_0 = 6.975$ mM [red line in Fig. 2(b)]. In scenario (i), i.e., local response approximation, the conversion efficiency peaks at the PB angle and at the angular positions of the three resonances associated with leaky modes [black line in Fig. 2(b)], following the average electric-field enhancement maxima shown in Fig. 2(a). We note however that largest SH conversion efficiency is achieved when exploiting leaky modes rather than the PB condition. When the nonlocal, free-electron gas pressure is taken into account [blue line in Fig. 2(b) corresponding to scenario (ii)], the SH conversion efficiency maxima are significantly damped and the positions of the peaks are shifted at larger angles with respect to the local approximation [black line - scenario (i)]. This is due to the fact that nonlocality introduces extra losses to the system. We then compensate the additional damping due to the electron gas pressure nonlocality by increasing the dye molecules concentration from $\bar{N}_0 = 6.75$ mM to $\bar{N}_0 = 6.975$ mM [red line - scenario (iii)]. The extra gain re-establishes conversion efficiencies peaks similar to those observed in the limit of the local approximation [black line - case (i)] without any angular shift with respect to case (ii), i.e., nonlocal contribution and smaller gain ($\bar{N}_0 = 6.75$ mM). Conversion efficiencies are six orders of magnitudes larger than conversion efficiency obtained for flat metal surfaces illuminated by TM-polarized light.

4. Conclusions

The inherent nonlocal response of metal dramatically reduces the average field enhancement in the ENZ slab and, as a consequence, inhibits SH generation. However, when additional gain is introduced in the system to compensate the effective damping due to the nonlocal term, the average field enhancement in the slab increases and simultaneously SH conversion efficiency is boosted.

5. References

1. M. A. Vincenti, D. de Ceglia, A. Ciattoni, and M. Scalora, "Singularity-driven second- and third-harmonic generation at ε-near-zero crossing points," Phys. Rev. A **84**, 063826 (2011).
2. A. Ciattoni and E. Spinozzi, "Efficient second-harmonic generation in micrometer-thick slabs with indefinite permittivity," Phys. Rev. A **85**, 043806 (2012).
3. S. Campione, D. de Ceglia, M. A. Vincenti, M. Scalora, and F. Capolino, "Electric field enhancement in ε-near-zero slabs under TM-polarized oblique incidence," Phys. Rev. B **87**, 035120 (2013).
4. R. E. Collin, *Field theory of guided waves* (McGraw Hill, 1960).
5. A. Alù, M. G. Silveirinha, A. Salandrino, and N. Engheta, "Epsilon-near-zero metamaterials and electromagnetic sources: Tailoring the radiation phase pattern," Phys. Rev. B **75**, 155410 (2007).
6. J. A. Gordon and R. W. Ziolkowski, "The design and simulated performance of a coated nano-particle laser," Opt. Express **15**, 2622-2653 (2007).
7. S. Campione, M. Albani, and F. Capolino, "Complex modes and near-zero permittivity in 3D arrays of plasmonic nanoshells: loss compensation using gain [Invited]," Opt. Mater. Express **1**, 1077-1089 (2011).
8. A. Boltasseva and H. A. Atwater, "Low-Loss Plasmonic Metamaterials," Science **331**, 290-291 (2011).
9. E. D. Palik and G. Ghosh, *Handbook of optical constants of solids* (Academic press, 1998), Vol. 3.
10. S. Y. Kim and K. Vedam, "Analytic solution of the pseudo-Brewster angle," J. Opt. Soc. Am. A **3**, 1772-1773 (1986).
11. M. Scalora, M. A. Vincenti, D. de Ceglia, V. Roppo, M. Centini, N. Akozbek, and M. J. Bloemer, "Second- and third-harmonic generation in metal-based structures," Phys. Rev. A **82**, 043828 (2010).
12. M. A. Vincenti, S. Campione, D. de Ceglia, F. Capolino, and M. Scalora, "Gain-assisted harmonic generation in near-zero permittivity metamaterials made of plasmonic nanoshells," New Journal of Physics **14**, 103016 (2012).